Volume 1 | Number 1 | Jan 2013 | Pages 1–100

Analytical Methods

www.rsc.org/methods

ROYAL SOCIETY OF CHEMISTRY

www.rsc.org/methods

Electrochemical sensor for sensitive determination of nitrites based on the Pt–PANI–graphene Nanocomposites

Sai Zhang, Bo-Qiang Li, Jian-Bin Zheng[*]

Institute of Analytical Science, Shaanxi Provincial Key Laboratory of

Electroanalytical Chemistry, Northwest University, Xi'an, Shaanxi 710069, China

A new sandwich structure nanocomposite of Pt nanoparticles supported on PANI modified graphene was synthesized and used for fabricating nitrite sensor. Morphology and composition of the nanocomposites were characterized by transmission electron microscope and X-ray diffraction. Electrochemical investigation indicated that the nanocomposites possess excellent electrochemical oxidation ability towards nitrites. The sensor exhibited two linear ranges: one from 0.4 μM to 0.99 mM with a correlation coefficient of 0.9974 and sensitivity of 485.5 $\mu A \cdot mM^{-1} \cdot cm^{-2}$; another from 0.99 mM to 7.01 mM with a correlation coefficient of 0.9981 and sensitivity of 154.3 $\mu A\ mM^{-1}\ cm^{-2}$. The limit of detection (LOD) of this sensing system was 0.13 μM at the signal-to-noise ratio of 3. Additionally, the sensor exhibited good reproducibility, long-term stability, and anti-interference.

Keywords: electrochemical sensor, graphene, polyaniline, nitrite

1. Introduction

Nitrite is considered to be a terrible pollutant to the human health and environment [1, 2] because it is widely present in the dye industry, food industry and other fields. It is reported that nitrite can interact the secondary amine to generate carcinogenic nitrosamines in human body [3].Thus exists a great potential safety hazard to the human health. Therefore it is very important for environmental protection and public health to the detection of nitrite. A lot of methods based on different principles have been developed to detect nitrite, such as chromatography [4],

[*]Corresponding author, e-mail: zhengjb@nwu.edu.cn

1   chemiluminescence [5], fluorescence [6] and electrochemistry methods [7]. Among

2   various methods for nitrite detection, electrochemical sensor has attracted

3   considerable attentions because it shows many advantages such as simple operation,

4   low cost, high sensitivity, and fast response. The oxidation of nitrite can directly occur

5   on the glassy carbon electrode (GCE), but its overpotential is very high, which limits

6   the sensitive and selective detection of nitrite. It is necessary to develop new

7   functional nanomaterials to promote the electron transfer and to lower the operating

8   potential for nitrite oxidation.

9   Among various materials, Graphene (GE) has attracted considerable attentions

10 thanks to its high specific surface area, the special electronic properties, strong

11 mechanical strength and perfect conductive. [8-10] Graphene shows above excellent

12 physical properties because of its single atomic plane of sp^2 carbon atom networks

13 [11-13]. Its excellent electron transfer property and large surface-to-volume ratio endow

14 graphene-based materials with large specific surface area [14, 15], perfect electrical

15 conductivity [16, 17], good biological compatibility, more catalytic activity center [18.19]

16 and so on. All kinds of graphene-based materials modified electrodes have been used

17 for detection of various kinds of biological molecules [20-22]. For instance, Sun et al [23]

18 reported the first graphene-based hydrogen peroxide biosensor with wide linear

19 responses, good reproducibility, and high stability.

20   Polyaniline (PANI) as a kind of conductive polymer, have been extensively used

21 in electrochemical sensing fields due to its simple synthesis, synthesis of low cost and

22 reversible redox properties [24-26]. Unfortunately, PANI usually suffers from a limited

23 long-term stability during cycling due to the degradation caused by swelling and

24 shrinking. In order to overcome the above problems, hybrid nanocomposite combined

25 with carbons has been widely studied in recent years. Numerous studies have found

26 that graphene (GE) and polyaniline can be linked together through π-π conjugate

27 steadily [27], which not only improves the easy agglomeration and poor solubility of

28 graphene, but also contribute to the existence of long-term stability of polyaniline.

29   Pt nanoparticles (PtNPs) have attracted considerable attentions in the

30 development of novel electrochemical sensors thanks to its large surface-to-volume

1 ratio and high electrocatalytic activity [28].

2   In this work, a kind of Pt–PANI–GE nanocomposites was firstly synthesized,

3 and then a nitrite electrochemical sensor based on the Pt–PANI–GE nanocomposites

4 was constructed and further applied in a real sample analysis.

2. Experimental section

2.1. Chemicals and material

7   High purity graphite powder with an average particle diameter of 4 mm was

8 purchased from Shanghai Carbon plant (Shanghai, China). Aniline was distilled under

9 vacuum to remove the oxidation impurities before using. H_2PtCl_6 (99%) was

10 purchased from Sinopharm Chemical Reagent Co. Ltd. (Shanghai,China).

11 Polyvinylpyrrolidone (PVP), hydrogen peroxide, ammonium persulfate (APS),

12 sodium nitrite and other reagents were of analytical reagent grade and doubly distilled

13 water was used in experiments. 0.1 M phosphate buffered saline (PBS, pH=6.0) was

14 used as the supporting electrolyte unless other stated.

2.2. Apparatus and measurements

16   X-ray diffraction (XRD) patterns of the samples were observed by D/MAX-3C

17 (Rigaku, Japan). The transmission electron microscope (TEM) image was carried out

18 by Tecnai G^2 F20 S-TWIN (FEI, USA). Electrochemical measurements were carried

19 out in a conventional three-electrode electroanalysis system controlled by CHI660

20 electrochemical workstation (Shanghai CH Instrument Co., Ltd., China). Glassy

21 carbon electrodes (3 mm in diameter) were used as a working electrode, saturated

22 calomel electrode (SCE) and platinum wire was used as the reference electrode and

23 counter electrode, respectively. All electrochemical experiments were carried out at

24 room temperature.

2.3. Preparation of the sensor

2.3.1. Synthesis of PANI

27   According to the previously report [29], the purified aniline (146 μL, 1.6 mmol)

28 and ammonium peroxydisulfate (APS, 91.2 mg, 0.4 mmol) in two beakers containing

1   10 mL of 0.5 M HCl, respectively. Afterwards, the APS solution was rapidly added

2   into the aniline solution and shaken vigorously for 40 s. Polymerization procedure

3   was carried out at 20℃ for 2 h.

2.3.2. Preparation of GO nanosheets

5   Graphene oxide (GO) was prepared from natural graphite powder by a modified

6   Hummers method [30]. Briefly, 1 g of graphite powder and 0.6 g $NaNO_3$were stirred in

7   30 mL of 98% H_2SO_4 for 4h. Then 4 g $KMnO_4$ was added while cooling to maintain

8   the mixture below 20℃. The mixture then stirred at 35-40℃ for 40 min，then at

9   65-80℃ for 50 min. Next 60 mL of distilled water was slowly added to the mixture

10   and heated at 98-105℃ for 20min. The reaction was terminated by adding 180 mL of

11   distilled water followed by 10 mL of 30% H_2O_2 solution. The product was collected

12   by centrifugation and washed repeatedly with 5% HCl solution and dried in vacuum at

13   60℃ overnight.

2.3.3. Preparation of PANI–GE nanoparticles

15   In a typical reaction, a 2 mg/mL GO dispersion was prepared by the sonication of

16   20 mg GO in 10 mL water for about 2 h, and 10 mL suspension (2 mg/mL) of PANI

17   was obtained as the same. Then the 10 mL GO dispersion and 80 mg PVP were added

18   into PANI suspension with further sonication for about 30min. The mixed solution

19   were transferred into a 25 mL Teflon-lined autoclave. After heating at 180℃ for 20 h

20   and naturally cooling to room temperature. The final product, denoted as PANI–GE.

21   composites, obtained by centrifuged, then washed with water and dried at 70 ºC

22   before characterization and application.

2.3.4. Preparation of Pt–PANI–GE nanocomposites

24   10 mg PANI–GE was dispersed in 15 mL water solution by ultrasonication for

25   30 min, 1 ml of 19.3 mM H_2PtCl_6 aqueous solution was added. After sonicating for

26   another 30 min, 10 ml $NaBH_4$ solution (24 mM) was added into the dispersion in a

27   dropwise manner under magnetic stirring. After stirring for 24h at room temperature,

28   the composite product was centrifuged and washed with doubly distilled water. The

29   obtained powder was dired at 60 ºC for 4 h.

1 2.3.5. Electrode modification

2 　　　The modified electrode was prepared by a simple casting method. First, the

3 GCE for each experiment was mechanically polished with 0.3 μm alumina powder to

4 obtain mirror like surface. After that, the electrode was successively washed in

5 ethanol solution and doubly distilled water for 3min by sonication method. Then, the

6 GCE was allowed to dry in a steam of nitrogen. The 1.5 mg nanocomposite was

7 dispersed into 1 ml doubly distilled water and sonicated for 30 minutes; 5 μL Pt

8 –PANI–GE suspension was cast onto the GCE and then dried in air at room

9 temperature (27 ℃).

10 **3. Results and discussion**

11 3.1. Characterization of Pt–PANI–GE nanocomposites

12 　　　The morphology and microstructure of as-prepared nanocomposites were

13 characterized by transmission electron microscope (TEM). Fig. 1A demonstrated

14 typical single monolayer structure of GO sheet, some folds were seen on the surface

15 of GO clearly. It was clearly seen from Fig. 1B, that Polyaniline was interwoven by

16 different lengths of nanowires, each the length of about 200 nm. Figure C and D were

17 Pt–PANI–GE TEM image. It was clearly observed that PANI was wrapped on the

18 surface of GE from the pictures, and also observed that spherical Pt nanoparticles

19 were uniformly deposited on PANI–GE surface. The particle diameter was only about

20 5nm. No PtNPs aggregation was observed, which may be because PANI-GE provides

21 a large specific surface area for Pt sufficient nucleation sites.

22

23 　　　　　　　　　　　　　　　　**Fig. 1.**

24

25 　　　Fig. 2 showed the XRD patterns of GO, PANI, PANI–GE and Pt–PANI–GE

26 nanocomposites, respectively. The GO sheets (curve a) showed a clear diffraction

27 peak at $2\theta = 10°$, which was due to the existence of aqueous solution in the

28 hydrophilic surface GO layer [31]. The pure polyaniline (curve b) showed a clear

29 diffraction at $2\theta = 25°$, which was consistent with (200) crystal plane of PANI in its

1 emeraldine salt [32]. PANI–GE (curve c) and Pt–PANI–GE (curve d) had emerged

2 PANI diffraction peaks, as compared to the PANI–GE, at $2\theta = 41°$, $47°$, $68°$ appeared

3 three new diffraction peak in curve of Pt–PANI–GE, which corresponded to the (111),

4 (200) and (220) crystallographic planes of PtNPs [33], respectively.

5

6 **Fig. 2.**

7

8 3.2. Mechanism of the Pt–PANI–GE formation

9   Based on the above experimental process and characterization, Fig.3 clarified the

10 preparation mechanism for the Pt–PANI–GE nanocomposites. As shown: First of all,

11 through polymerization generated polyaniline at room temperature. Then PANI, GO

12 and PVP suspension was then transferred into a Teflon-lined autoclave and reacted at

13 180ºC for 20 h. At high temperature, the reduction took place with PVP as reducing

14 agent, GO was reduced to GE, and PANI through π-π interactions connected with GE.

15 In the presence of PANI, the PANI–GE could offer more active area for Pt dispersing.

16 The H_2PtCl_6 solution was introduced into the suspension of PANI–GE and mixed

17 uniformly under ultrasonicating condition, $PtCl_6^{2-}$ wrapped around and formed layer

18 on PANI–GE surface during the sonication. Then the reduction took place with

19 NaBH4 as reducing agent and continuous magnetic stirring, and finally, well

20 dispersed PtNPs supported on PANI–GE were obtained.

21

22 **Fig. 3.**

23

24

25 3.3. Electrochemical properties of Pt–PANI–GE

26   Electrochemical impedance spectroscopy (EIS) was a common and effective

27 method for studying interfacial properties of the working electrode. The results of

28 different modified electrodes were shown in Fig. 4A. Bare GCE had a large semicircle

29 diameter (curve a), implying its obstructive role to electron transfer in electrolyte

solution. When GO was modified onto the electrode surface, compared to the bare electrode, the semicircle diameter of GO/GCE (curve b) was further larger, Showing that GO played a certain insulation blocking the electron transfer due to destruction of its sp^2 bonding networks [34]. The semicircle diameter of PANI–GE/GCE (curve c) was significantly smaller than that of the GO/GCE, which was mainly due to two reasons: at high temperature, GO was reduced to GE, reinforced its electrical conductive; another reason was PANI having a good electrical conductivity. When Pt was immobilized onto PANI–GE, The semicircle diameter of Pt–PANI–GE/GCE was reduced owing to the good conductivity of Pt NPs that promoted the electron transfer.

Fig. 4.

The electrocatalytic performance of different modified electrodes toward the oxidation of nitrite were studied by cyclic voltammetry(CV). Figure.4 B illustrated the CV behaviors of the bare GCE (a), GO/GCE (b), PANI–GE/GCE (c) and (d) Pt–PANI–GE/GCE in 0.10 M phosphate buffer (pH 6.0) solution containing 1.0 mM nitrite at the scan rate of 50 mV s^{-1}. No current response was observed at the GO/GCE (curve b), the reason was GO act as an insulating layer that hinder the electron transfer [35]. In comparison with that of the bare GCE (a), the oxidation current response of PANI–GE/GCE (curve c) had obvious larger. The reason was that PANI–GE has big area and good electrical conductivity, which was advantageous to the electron transfer. When Pt was immobilized onto PANI–GE, compared with PANI–GE/GCE, the oxidation current response of Pt–PANI–GE/GCE (curve d) were increased 35 μA. The reason was owing to the good conductivity of Pt NPs that accelerated electron transfer.

The CVs of the Pt–PANI–GE/GCE in different concentrations of nitrite were also measured in Fig. 5A. It can be seen that no characteristic peak was appeared when no nitrite was added into the system. Along with adding different concentrations of nitrite, the oxidation peak current appeared and gradually increased, and showed a good linear relationship (Figure5.A inset) between peak current and concentration. This indicated that Pt–PANI–GE nanocomposites have good electrocatalytic activity

toward nitrites.

Fig. 5.

Figure 5B exhibited the CVs of Pt–PANI–GE/GCE gaining 4.0 mM nitrite at different scan rates. As the scan rate increased, the peak currents also increased, and the oxidation peak current increased linearly with the square root of the scan rate (Figure 5B inset), which proved nitrite in the modified electrode surface catalytic oxidation reaction was controlled by diffusion [36].

To improve the performance of the sensor, we optimized the pH value of 0.1 M PBS by testing the CVs of the Pt–PANI–GE/GCE toward 1.0 mM NO_2^-. As it was clearly shown in Fig. 6, with the increase of pH peak, current also increased, until reach maximum at pH = 6.0, but in the pH range of 6.0 ~ 9.0, with the increase of pH the peak current decreased. The reason for this phenomenon could be attributed to when pH <6.0, NO_2^- could not be stable, it would quickly break down into NO_3^- [37, 38], In contrast, nitrite oxidation became more difficult when the pH was above 7.0 (up to 9.0), owing to the lack of protons [39, 40]. Thus, pH = 6 was selected as the optimum pH value in our experiments. Therefore, the electrocatalytic oxidation mechanism for nitrite oxidation can be proposed:

$$H^+ + NO_2^- \leftrightarrow HNO_2 \tag{1}$$

$$NO_2^- \leftrightarrow NO_2 + e^- \tag{2}$$

$$2NO_2 + H_2O \leftrightarrow 2H^+ + NO_2^- + NO_3^- \tag{3}$$
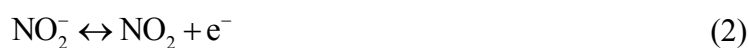
Fig. 6.

Fig. 7A showed the amperometric current–time curve of the Pt–PANI–GE/GCE under 0.75 V with successive additions of nitrite. With different concentrations of nitrites were added into a continuous stirring PBS, Pt–PANI–GE/GCE responded for matrix quickly. It took less than 3 s to achieve the steady-state current, indicating that the sensor has good catalytic activity toward nitrite. The calibration curve for the

nitrite sensor was shown in the Fig.7B. The Pt–PANI–GE/GCE gave two linear

dependence in the nitrite concentration ranges: one from 0.4 μM to 0.99 mM, linear

regression equation was Ip (μA) = 0.150 + 34.3C (mM) with the correlation

coefficient of 0.9974 and sensitivity of 485.5 $\mu A \cdot mM^{-1} \cdot cm^{-2}$; another from 0.99 mM

to 7.01 mM, linear regression equation was Ip (μA) = 22.7+10.9·C (mM) with the

correlation coefficient of 0.9981 and sensitivity of 154.3 $\mu A\ mM^{-1}\ cm^{-2}$. The limit of

detection (LOD) of this sensing system was 0.13 μM at the signal-to-noise ratio of 3.

Compared with some other modified electrodes listed in Table 1, the results indicated

that the proposed Pt–PANI–GE/GCE may be an excellent platform for

electrochemical detection of nitrite. The reasons of two linear curves were shown

below: in the low concentration range, nitrite spreads to the modified electrode

surface and reacted quickly, the response current was large; in high range, while

mixing had been accompanied by the whole reaction process, but in the process of

reaction, electrode surface inevitably produced the adsorption, resulting in nitrite

diffusion hindered. So the small response current generated in a high concentration

range and the sensitivity was low.

Fig. 7.

Table1.

3.4. Reproducibility, stability and anti-interference performance of Pt–PANI–GE/GCE

Under optimal conditions, the anti-interference advantage of the

Pt–PANI–GE/GCE was studied by using amperometric method. As was shown in Fig.

8, 0.5mM $NaNO_2$, Na_2SO_4, KCl, KNO_3, $KClO_4$ and $CuCl_2$ were continuously added

into the solution, the result showed that the interfering substance almost had little

effect on the detection of nitrite. The above results showed that Pt–PANI–GE/GCE

possess perfect anti-interference abilities for detecting nitrite.

Fig. 8.

In order to study the repeatability of the applied electrode, the same electrode was used for detecting the same concentration of $NaNO_2$ six times in a row by cyclic voltammetry, the oxidation current standard deviation was 3.42%. This result indicated that the sensor has good reproducibility for detection of nitrite. When the modifed electrode was stored at 4 ºC for a month, for the same concentration $NaNO_2$, its current response was approximately 92% of the initial value, which showed that the sensor has a good stability for detection of nitrite.

3.5. Application

In order to assess the practical applications of the sensor, we use the standard addition method to detect nitrite in tap water by amperometric detection methods. The sample was dissolved in 0.1 mol • L^{-1} PBS (pH = 6) solution for testing, the results were shown in Table 2. As seen from the table, the recovery was 104.2%, 99.1% and 100.7%, respectively. Relative standard deviation (RSD) was 2.3%, 1.9% and 2.6%, respectively. The result indicated that the sensor can be applied to detect the actual sample.

Table 2.

4. Conclusions

In summary, Pt–PANI–GE nanocomposites were synthesized successfully and used for constructing a novel nitrite sensor. The sensor showed high electrocatalytic activity toward nitrites and many excellent features such as wide linear range, long-term storage stability, high sensitivity, satisfactory anti-interference ability, and high reproducibility. This research could provide a reference for the study of electrochemical sensing conductive graphene-based polymer nanocomposites.

References

[1]   N. S. Bryan, Free Radical Biol. Med., 2006, 41, 691.

[2]   W. Lijinsky and S. S. Epstein, Nature, 1970, 225, 21.

[3]   S. S. Mirvish, Cancer Lett., 1995, 93, 17.

[4]   A. Gáspár, P. Juhász and K. Bágyi, J. Chromatogr. A, 2005, 1065, 327.

[5]   Z. Lin, W. Xue, H. Chen and J. Lin, Anal. Chem., 2011, 83, 8245.

[6]   H. Li, C. J. Meininger and G. Wu, J Chromatogr. B Biomed. Appl., 2000, 746, 199.

[7]   M. Muchindu, T. Waryo, O. Arotiba, E. Kazimierska, A. Morrin, A. J. Killard, M. R. Smyth, N. Jahed, B. Kgarebe, P. G. L. Baker and E. I. Iwuoha, Electrochim. Acta, 2010, 55, 4274.

[8]   J. Zhang, F. Zhao, Z. P. Zhang, N. Chen and L. T. Qu, Nanoscale, 2013, 5, 3112.

[9]   J. Q. Ling, W. T. Zhai, W. W. Feng, B. Shen, J. F. Zhang, and W. G. Zheng, ACS Appl. Mater. Inter., 2013, 5, 2677.

[10] H. P. Cong, J. F. Chen and S. H. Yu, Chem. Soc. Rev., 2014, 43, 7295.

[11] G. He, H. Chen, J. Zhu, F. Bei, X. Sun and X. Wang, J. Mater. Chem., 2011, 21, 14631.

[12] D. Li and R. B. Kaner, Nat. Nanotechnol., 2008, 3, 101.

[13] A. K. Geim, and K. S. Novoselov, Nat. Mater., 2007, 6, 183.

[14] M. D. Stoller, S. Park, Y. Zhu, J. An and R. S. Ruoff, Nano Lett., 2008, 8, 3498.

[15] S. Park and R. S. Ruoff, Nat. Nanotechnol., 2009, 4, 217.

[16] K. S. A. Novoselov, A. K. Geim, S. V. Morozov, D. Jiang, M. I. Katsnelson, I. V. Grigorieva, S. V. Dubonos and A. A. Firsov, Nature, 2005, 438, 197.

1 [17] Y. Zhang, Y. Tan, H. L. Stormer and P. Kim, Nature, 2005, 438, 201.

2 [18] H. Teymourian, A. Salimi and S. Khezrian, Biosens. Bioelectron., 2013, 49, 1.

3 [19] H. Liu, J. Gao, M. Xue, N. Zhu, M. Zhang and T. Cao, Langmuir, 2009, 25, 12006.

4 [20] W. J. Lin, C. S. Liao, J. H. Jhang and Y. C. Tsai, Electrochem. Commun., 2009, 11, 2153.

5 [21] Y. Chen, Y. Li, D. Sun, D. Tian, J. Zhang and J. Zhu, J. Mater. Chem., 2011, 21, 7604.

6 [22] F. Xu, M. Deng, Y. Liu, X. Ling, X. Deng and L. Wang, Electrochem. Commun., 2014, 47,

7   33.

8 [23] J. Sun, K. Huang, S. Zhao, Y. Fan and Z. Wu, Bioelectrochem., 2011, 82, 125.

9 [24] K. Zhang, L. Zhang, X. Zhao and J. Wu, Chem. Mater., 2010, 22, 1392.

10 [25] K. Wang, H. Wu, Y. Meng and Z. Wei, Small, 2014, 10, 14.

11 [26] Y. Zhou, Z. Qin, L. Li, Y. Zhang, Y. Wei, L. Wang and M. Zhu, Electrochim. Acta, 2010, 55,

12   3904.

13 [27] J. Zhang and X. Zhao, The J. Phys. Chem. C, 2012, 116, 5420.

14 [28] D. Yuan, S. Chen, F. Hu, C. Wang and R. Yuan, Sens. Actuators B: Chemical, 2012, 168,

15   193.

16 [29] D. Li and R. B. Kaner, J. Am. Chem. Soc., 2006, 128, 968.

17 [30] D. C. Marcano, D. V. Kosynkin, J. M. Berlin, A. Sinitskii, Z. Sun, A. Slesarev, L. B.

18   Alemany, W. Lu and J. M. Tour, ACS Nano, 2010, 4, 4806.

19 [31] M. Z. Kassaee, E. Motamedi and M. Majdi, Chem. Eng. J., 2011, 172, 540.

20 [32] F. Yang, M. Xu, S. Bao, H. Wei and H. Chai, Electrochim. Acta, 2014, 137, 381.

21 [33] Z. Li, L. Zhang, X. Huang, L. Ye and S. Lin, Electrochim. Acta, 2014, 121, 215.

22 [34] Y. Hu, F. Li, X. Bai, D. Li, S. Hua, K. Wang and L. Niu, Chem. Commun., 2011, 47, 1743.

23 [35] S. Basu and P. Bhattacharyya, Sens. Actuators B: Chemical, 2012, 173, 1.

24 [36] D. Ning, H. Zhang and J. Zheng, J. Electroanal. Chem., 2014, 717, 29.

25 [37] B. Piela and P. K. Wrona, J. Electrochem. Soc., 2002, 149, E55.

26 [38] X. Xing and D. A. Scherson, Anal. Chem., 1988, 60, 1468.

27 [39] B. R. Kozub, N. V. Rees and R. G. Compton, Sens. Actuators B: Chemical, 2010, 143, 539.

28 [40] Z. Meng, B. Liu, J. Zheng, Q. Sheng and H. Zhang, Microchim. Acta, 2011, 175, 251.

29 [41] S. Zhao, K. Zhang, Y. Sun and C. Sun, Bioelectrochem., 2006, 69, 10.

30 [42] P. Wang, F. Li, X. Huang, Y. Li and L. Wang, Electrochem. Commun., 2008, 10, 195.

Analytical Methods

1 [43]   P. Miao, M. Shen, L. Ning, G. Chen and Y. Yin, Anal. Bioanal. Chem., 2011, 399, 2407.

2 [44]   V. Mani, A. P. Periasamy and S. Chen, Electrochem. Commun., 2012, 17, 75.

3

4 **Figure captions:**

5 **Fig. 1.** TEM images of (A) GO (B) PANI–GE (C, D) Pt–PANI–GE.

6 **Fig. 2.** XRD patterns of GO(a), PANI(b), PANI–GE(c), Pt–PANI–GE(d).

7 **Fig. 3.** The mechanism formed Pt–PANI–GE.

8 **Fig. 4.** (A) Electrochemical impedance spectra of Bare(a), GO/GCE(b),

9 PANI–GE/GCE(c), Pt–PANI–GE/GCE(d) in a 0.1 M KCl solution containing 5 mM

10 $K_3[Fe(CN)^6]/K_4[Fe(CN)^6]$. (B) CVs of bare(a), GO/GCE(b), PANI–GE/GCE(c),

11 Pt–PANI–GE/GCE(d) in 0.1 M PBS (pH 6.0) in the presence of 1.0 mM NO_2^-. scan

12 rate: 50 mV·s^{-1}.

13 **Fig. 5.** (A) Cyclic voltammograms obtained Pt–PANI–GE/GCE in N_2-saturated pH

14 7.2 PBS in the presence of NO_2^- with different concentrations (from a to i: 0, 0.5, 1.0,

15 1.5, 2.0, 2.5, 3.0, 3.5 and 4.0 mM) at a scan rate of 50 mV/s. (B) Cyclic

16 voltammograms obtained Pt–PANI–GE/GCE in N_2-saturated pH 7.2 PBS contained

17 4.0 mM NO_2^- at different scan rates (from a to j: 20, 40, 60, 80, 100, 120, 140, 160,

18 180 and 200 mV/s). Inset: plot of electrocatalytic peak current of NO_2^- versus $v^{1/2}$.

19 **Fig. 6.** Effect of solution pH on the oxidation current of 1.0 mM NO_2^- at

20 Pt–PANI–GE/GCE in 0.1 M PBS.

21 **Fig. 7.** (A) Amperometric curve obtained Pt–PANI–GE/GCE for successive additions

22 of NO_2^- in N_2-saturated pH 7.2 PBS at the work potential of 0.75 V under constant

23 stirring. (B) Calibration curve of NO_2^- versus its concentration.

24 **Fig. 8.** Amperometric response of $NaNO_2$, Na_2SO_4, KCl, KNO_3, $KClO_4$ and $CuCl_2$

25 (0.05 mM, respectively) on Pt–PANI–GE/GCE in N_2-saturated pH 7.2 PBS at the

26 work potential of 0.75 V under constant stirring.

27

28

29

30

1

2

3

4 **Fig. 1.**
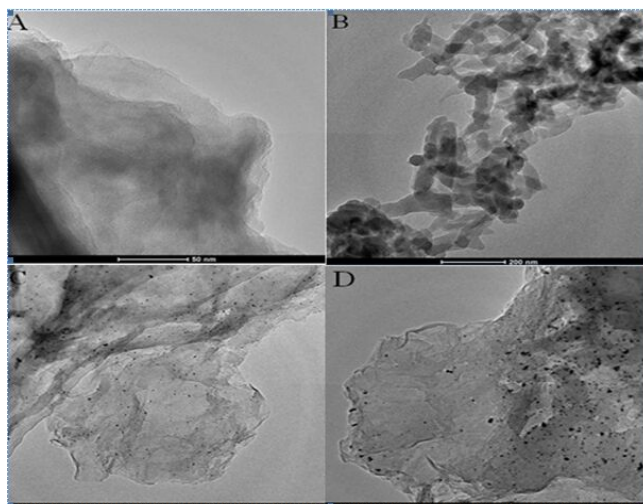
5

6

7

8 **Fig. 2.**

9

10 **Fig. 3.**

14
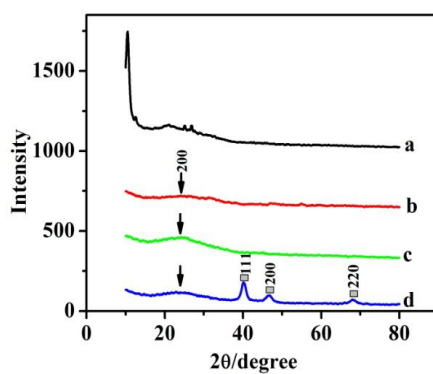
1
2
3
4
5
6
7
8
9
10
11
12
13
14
15
16
17
18

1

19
20　　2
21
22　　3　**Fig. 4.**
23
24　　4
25
26
27
28
29
30
31
32
33
34
35

36　　5
37
38　　6
39
40　　7　**Fig. 5.**
41
42
43
44
45
46
47
48
49
50
51

52　　8
53
54　　9
55
56　10
57
58　11　**Fig. 6.**
59
60
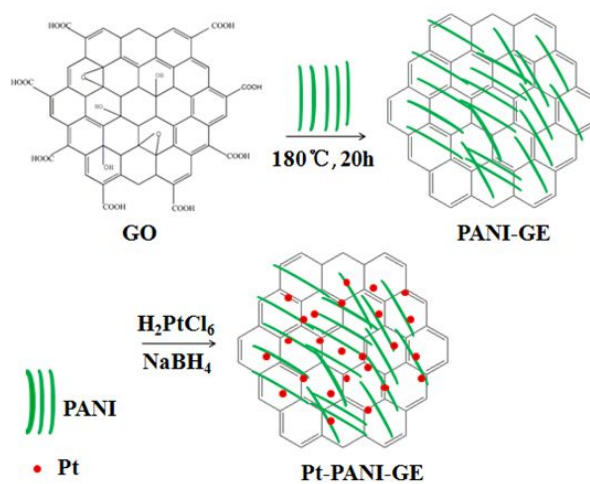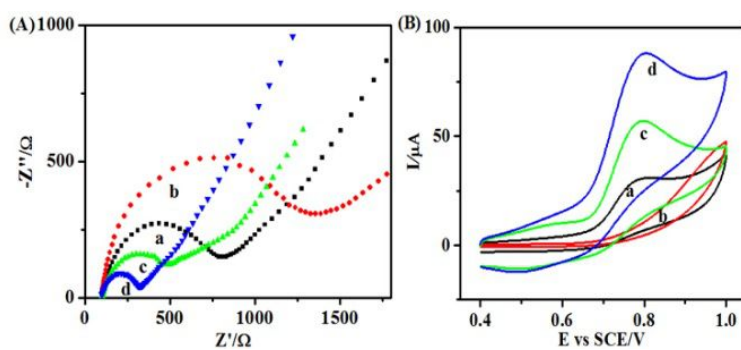
1
2
3
4
5
6 **Fig. 7.**

7
8
9
10 **Fig. 8.**

11
12
13

16
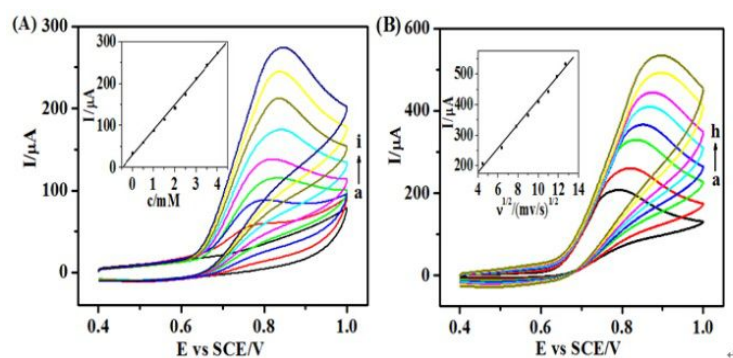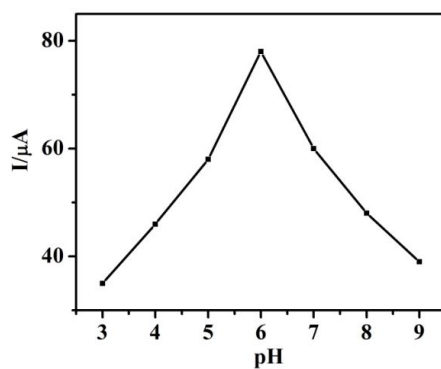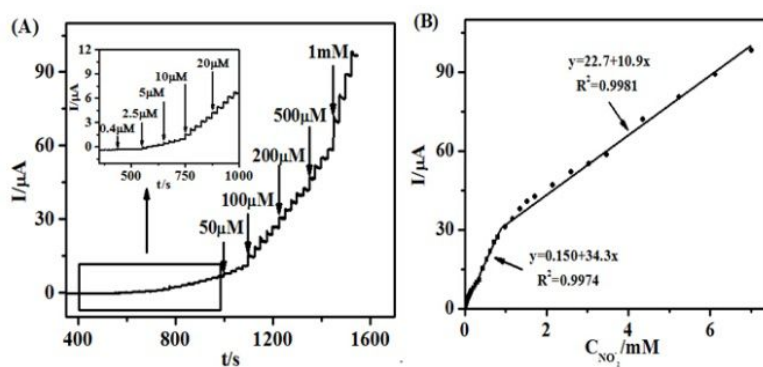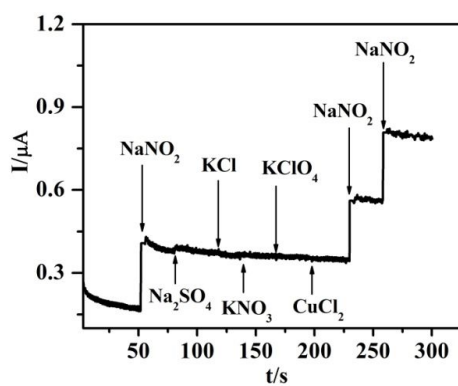
Table 1. Comparison of several electrochemical sensors for NaNO$_2$ determination

Sensors	Applied potential (V)	Linear range (μM)	Sensitivity	Detection limit (μM)	Literature
GCE	–	2.5–10	36μA mM^{-1}	0.4	[39]
Hb[a]/Ag/TiO$_2$/GCE	0.987	2000–6000	5.84μA mM^{-1} cm^{-2}	34	[41]
Ag–PAMAM[b]/GCE	0.80	4–1440	265μA mM^{-1} cm^{-2}	0.4	[36]
Pt nanoclusters/GCE	0.82	1.2–900	–	0.4	[42]
Pt NPs/Au electrode	–	10–1000	–	5	[43]
CR–GO[c]/GCE	0.80	8.9–167	26.7μA mM^{-1}	1.0	[44]
Pt–PANI–GE/GCE	0.75	0.4-990.0 / 990.0-7010.0	485.5μA mM^{-1} cm^{-2} / 154.3μA mM^{-1} cm^{-2}	0.13	This work

[a] Hemoglobin.

[b] Polyamidoamine.

[c] Chemically reduced graphene oxide.

Table 2. Detection of NaNO$_2$ in real tap water samples using Pt–PANI–GE/GCE

Tap water sample	Added/μM	Founded/μM	Recovery/%	RSD/%
1	5.0	5.21	104.2	2.3
2	15.0	14.86	99.1	1.9

	3	30.0	30.22	100.7	2.6

1

Eletrochemical sensing of nitrites based on novel Pt–PANI–graphene nonocomposites